Fluorescent Probes Hot Paper

How to cite: *Angew. Chem. Int. Ed.* **2022,** *61,* e202116782
International Edition: doi.org/10.1002/anie.202116782
German Edition: doi.org/10.1002/ange.202116782

A Chemical Biology Toolbox Targeting the Intracellular Binding Site of CCR9: Fluorescent Ligands, New Drug Leads and PROTACs

*Max E. Huber, Lara Toy, Maximilian F. Schmidt, Hannah Vogt, Julian Budzinski, Martin F. J. Wiefhoff, Nicole Merten, Evi Kostenis, Dorothee Weikert, and Matthias Schiedel**

Abstract: *A conserved intracellular allosteric binding site (IABS) has recently been identified at several G protein-coupled receptors (GPCRs). Starting from vercirnon, an intracellular C–C chemokine receptor type 9 (CCR9) antagonist and previous phase III clinical candidate for the treatment of Crohn's disease, we developed a chemical biology toolbox targeting the IABS of CCR9. We first synthesized a fluorescent ligand enabling equilibrium and kinetic binding studies via NanoBRET as well as fluorescence microscopy. Applying this molecular tool in a membrane-based setup and in living cells, we discovered a 4-aminopyrimidine analogue as a new intracellular CCR9 antagonist with improved affinity. To chemically induce CCR9 degradation, we then developed the first PROTAC targeting the IABS of GPCRs. In a proof-of-principle study, we succeeded in showing that our CCR9-PROTAC is able to reduce CCR9 levels, thereby offering an unprecedented approach to modulate GPCR activity.*

G protein-coupled receptors (GPCRs) are among the most relevant protein families in drug discovery and are the targets for approximately one third of all available medication. The vast majority of the reported GPCR ligands bind to an orthosteric site that is located within the helical bundle and accessible from the extracellular environment. Apart from the orthosteric site, a highly conserved intracellular allosteric binding site (IABS) that enables the binding of small molecule antagonists has recently been identified by X-ray co-crystallography for the chemokine receptors CCR2,[1] CCR7,[2] CCR9[3] as well as for the beta-2 adrenergic receptor (β_2AR).[4] Moreover, a druggable IABS has been suggested for several other GPCRs.[5] Ligands targeting this allosteric binding site feature a new dual mechanism of specific GPCR modulation, which is characterized by i) stabilization of the inactive receptor conformation and ii) sterically blocking intracellular transducer action, i.e. G protein and/or β-arrestin binding.[1–4] Thus, targeting the IABS opens new opportunities to modulate receptor activity and to generate selectivity. Furthermore, the IABS enables the implementation of novel intracellular drug-targeting strategies, such as chemically induced protein degradation by means of proteolysis targeting chimeras (PROTACs). Due to their bivalent nature PROTACs enable the recruitment of an intracellular E3 ubiquitin ligase to the targeted protein, thereby inducing its ubiquitination and subsequent proteasomal degradation (Figure S1). Thus, the availability of intracellular GPCR ligands lays an essential foundation for the rational development of GPCR-targeted PROTACs.

Vercirnon (**1**, Figure 1A) is the intracellular antagonist that was co-crystallized with CCR9.[3] It features an outstanding selectivity for CCR9 (>1000-fold)[6] and progressed to phase III clinical trials for the treatment of Crohn's disease, thereby highlighting the high therapeutic potential of intracellular CCR9 antagonists. However, during phase III clinical trials, **1** failed to recapitulate the highly promising results from prior preclinical and clinical studies because of limited therapeutic efficacy.[7] Thus, new approaches to improve the therapeutic efficacy of intracellular CCR9 antagonism are urgently needed.

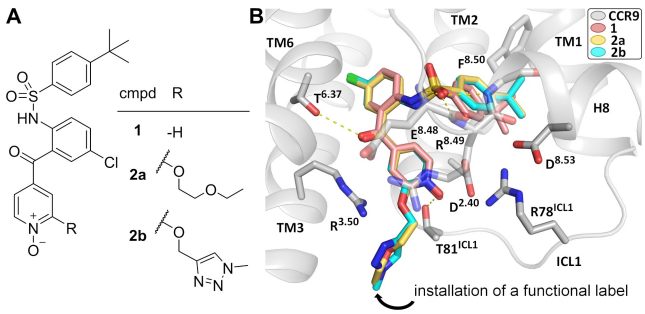

Figure 1. Design of heterobifunctional CCR9 ligands. A) Chemical structure of vercirnon (**1**) and the vercirnon-linker-conjugates (**2a**,**b**) that were identified by molecular docking as suitable templates for the design of heterobifunctional CCR9 ligands. B) Overlay of the reported binding mode of **1** (PDB ID: 5LWE)[3] with the predicted binding modes for **2a** and **2b**.

[*] M. E. Huber, L. Toy, M. F. Schmidt, H. Vogt, Dr. J. Budzinski, Dr. D. Weikert, Dr. M. Schiedel
Department of Chemistry and Pharmacy
Medicinal Chemistry
Friedrich-Alexander-Universität Erlangen-Nürnberg (FAU), Nikolaus-Fiebiger-Straße 10, 91058 Erlangen (Germany)
E-mail: matthias.schiedel@fau.de
M. F. J. Wiefhoff, Dr. N. Merten, Dr. E. Kostenis
Molecular, Cellular and Pharmacobiology Section
Institute for Pharmaceutical Biology
University of Bonn, Nussallee 6, 53115, Bonn (Germany)

For the discovery of new lead structures for intracellular GPCR modulators, molecular tools to study intracellular target engagement are crucial. The radioligand [^{3}H]vercirnon has already been established as a molecular tool to study binding to the IABS of CCR9 in a cell-free setup.[3] However, radioligand binding assays are accompanied by several drawbacks, such as high infrastructure requirements according to radiation protection measures, radioactive waste production, and heterogeneous assay protocols. The latter, is also the reason why radioligand binding assays do not allow a continuous readout and are not well-suited for detecting low affinity binders, such as fragments.

In order to provide a non-isotopic molecular tool to directly monitor binding to the IABS of CCR9 under cell-free conditions and, more importantly, in a cellular setup, we aimed to develop a fluorescently labeled vercirnon analogue. Molecular docking of vercirnon-linker conjugates (**2a**,**b**, Figure 1, Table S1) helped us to identify position 2 at the pyridine-*N*-oxide as a suitable vector for the installation of an alkoxy linker, which allows the conjugation of **1** with a functional label (Figure 1B), such as a cell-permeable tetramethylrhodamine (TAMRA) fluorophore. To enable a straightforward conjugation of the vercirnon scaffold with the TAMRA fluorophore via Cu-catalyzed Huisgen cycloaddition,[8] triazole-based linker fragments were included in the design and synthesis (Scheme S1) of the fluorescent CCR9 ligands. In order to evaluate the binding affinities of the synthesized fluorescent probes, we developed a NanoBRET-based binding assay (Figure S2). Therefore, we labeled CCR9 at its intracellular C-terminus with a small and bright luciferase variant (nanoluciferase, Nluc).[9] In a saturation binding experiment using membranes from HEK293T cells transiently expressing Nluc-tagged CCR9 (hereafter referred to as CCR9_Nluc), **3a** with its relatively short linker fragment showed the highest binding affinity ($K_d = 41.3 \pm 3.7$ nM, $pK_d = 7.39$, Figure 2A, B) among the tested ligands (**3a**–**d**, Table S2).

Kinetic binding studies with **3a** gave rate constants of $k_{on} = 4.79 \pm 0.48 \times 10^{-4}$ nM^{-1} min^{-1} and $k_{off} = 1.12 \pm 0.03 \times 10^{-2}$ min^{-1}, which resulted in a kinetic K_d value of 23.4 ± 2.4 nM ($pK_d = 7.63$, Figure 2C). The long residence time of **3a** ($t_r = 90.0 \pm 2.4$ min) indicates that the vercirnon scaffold might gain its high affinity and selectivity for CCR9 by slow off-kinetics. This is consistent with other literature examples for highly potent and selective compounds.[10]

In a displacement experiment with **3a**, a K_i value of 2.35 nM ($pK_i = 8.66 \pm 0.07$) was detected for **1** (Figure 2D; Table 1), which is in good agreement with published affinity data ($K_d = 0.49$ nM ($pK_d = 9.31$, radioligand binding assay); $K_i = 1.1$ nM ($pK_i = 8.96$, GPCR-activity assay)).[3,11] The orthosteric CCR9 agonist CCL25 did not affect the binding of **3a** to the IABS (Figure S3), which is consistent with reports for the related CCR2,[12] confirming non-competitive binding of intracellular allosteric antagonists. To investigate the suitability of our NanoBRET assay for future fragment-based drug discovery approaches, we tested several fragments (**4**–**9**) of **1** for competition with **3a**. Four of the tested fragments were identified as hits (inh. > 50 % @ 3.3 mM; Figure 2E) and were further characterized. The detected pK_i values indicate that the 4-(*tert*-butyl)-*N*-phenylbenzenesulfonamide moiety is critical for CCR9 binding (Figure S4).

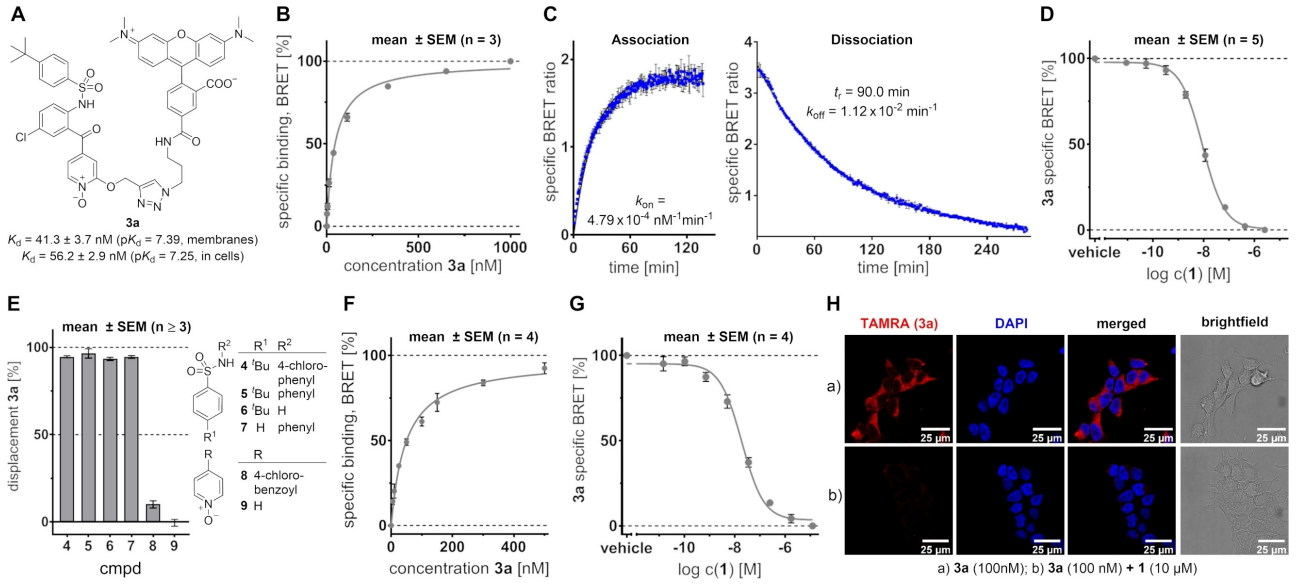

Figure 2. Development of **3a** as a fluorescent tool to target the IABS of CCR9. A) Chemical structure and equilibrium dissociation constants of **3a**. B) Binding curve of **3a** in a NanoBRET-based saturation experiment using CCR9_Nluc membranes. C) Representative association and dissociation curves with **3a** (100 nM) using CCR9_Nluc membranes. D) Competition binding curve for **1** obtained with **3a** (100 nM) and CCR9_Nluc membranes. E) Displacement of **3a** (100 nM) by fragments **4**–**9** (3.3 mM). See Figure S4 for detected pK_i values and Schemes S2, S3 for fragment synthesis. F) Binding curve of **3a** in a NanoBRET-based saturation experiment performed with live HEK293T cells expressing CCR9_Nluc. G) Competition binding curve for **1** obtained with **3a** (120 nM) and live HEK293T cells expressing CCR9_Nluc. H) Intracellular uptake of **3a** (100 nM) and displacement by **1** (10 µM) monitored by fluorescence microscopy.

Table 1: pK_i and pIC_{50} values [mean ± SEM, $n \geq 3$] of intracellular CCR9 antagonists **10–12** compared to **1**. K_i and IC_{50} values are given in brackets. For competition and inhibition curves see Figures S9, S10.

Compound	pK_i (K_i) NanoBRET (membranes)	pK_i (K_i) NanoBRET (in cells)	pIC_{50} (IC_{50}) Gα_o activation	pIC_{50} (IC_{50}) β-arrestin2 recruitment
1 (vercirnon)	8.66 ± 0.07 (2.35 nM)	8.24 ± 0.05 (5.93 nM)	8.40 ± 0.03 (3.99 nM)	7.70 ± 0.06 (20.2 nM)
10	8.49 ± 0.08 (3.51 nM)	7.98 ± 0.09 (11.5 nM)	7.83 ± 0.08 (14.9 nM)	7.76 ± 0.10 (17.4 nM)
11	7.91 ± 0.07 (13.0 nM)	7.72 ± 0.08 (20.5 nM)	6.59 ± 0.03 (256 nM)	6.78 ± 0.20 (166 nM)
12	9.30 ± 0.09 (0.53 nM)	8.86 ± 0.15 (1.91 nM)	8.72 ± 0.10 (1.92 nM)	8.71 ± 0.06 (1.93 nM)

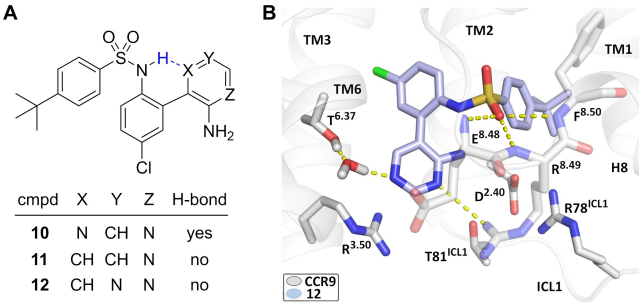

cmpd	X	Y	Z	H-bond
10	N	CH	N	yes
11	CH	CH	N	no
12	CH	N	N	no

Figure 3. Design of novel intracellular CCR9 antagonists. A) Chemical structure of the CCR9 antagonist **10** as reported by Zhang et al.[13] and its derivatives **11**, **12** that cannot form an intramolecular H-bond (see Figure S8). B) Molecular interactions of **12** (blue) with the IABS of CCR9 (grey), predicted by means of molecular dynamics simulation.

In a cell-based assay setup using HEK293T cells transiently transfected with CCR9_Nluc, a K_d value of 56.2 ± 2.9 nM (pK_d = 7.25) for **3a** was determined (Figure 2F), demonstrating that **3a** is indeed able to pass the cell membrane and bind to CCR9 on the intracellular side of the receptor. In a cell-based displacement assay, we detected a K_i value of 5.9 nM (pK_i = 8.24 ± 0.05) for **1** (Figure 2G, Table 1), which is consistent with the affinity data detected with our membrane-based setup (see above). Thus, **3a** is a suitable tool to study target engagement for the IABS of CCR9 in a cellular environment. In contrast, binding assays based on radiolabeled [^{3}H]vercirnon have only been described in a cell-free setup.[3]

Intracellular CCR9 binding of **3a** and its displacement by **1** was also monitored by fluorescence microscopy (Figure 2H, S5–S7). Thus, **3a** represents an unprecedented tool that enables visualization of ligand binding to the IABS of CCR9 in a cellular environment.

In a next step, we aimed to demonstrate suitability of our NanoBRET-based screening platform for the identification of novel intracellular CCR9 ligands. Following the hypothesis that the binding process of **1** to CCR9 is enthalpically hindered by an intramolecular H-bond, which is predicted to be present in solution (Figure S8) but not observed in the bioactive CCR9-bound conformation of **1** (Figure 1B),[3] we aimed to develop vercirnon derivatives that cannot form such an unfavourable intramolecular H-bond. As a starting point, we used the pyrazine-based vercirnon analogue **10** reported by Zhang et al.[13] According to our conformational analysis, this compound is also able to form an intramolecular H-bond. In contrast, the pyridine- and pyrimidine-based analogues **11** and **12** should not be able to form this unfavourable intramolecular H-bond, due to the removal or relocation of the H-bond accepting nitrogen atom (Figure 3, S8).

Analogues **10**, **11**, and **12** were synthesized (Scheme S3) and tested for their CCR9-binding affinity using our NanoBRET-based assay. Whereas the pyridine-based **11** showed reduced binding compared to **1** or **10**, compound **12** with its pyrimidine moiety yielded a significantly improved affinity in the membrane-based setup and in living cells (Table 1).

The increased affinity of **12**, compared to **1** and **10**, strengthens our initial hypothesis that the bioactive conformation of **1** is destabilized by an intramolecular H-bond. The difference in affinity between **11** and **12** might be rationalized by a water-mediated H-bond interaction with $T^{6.37}$ (according to Ballesteros-Weinstein numbering[14]) of CCR9. According to our modeling studies, an H-bond interaction with $T^{6.37}$, which has been observed for **1** (Figure 1B), can also be formed by **10** and **12**, but not by **11**, as this analogue lacks an H-bond donor in position 4 or 5 of the 2-aminopyridin moiety (Figure 3, S8). By means of CCR9 G protein activation and β-arrestin recruitment assays, we show that the improved affinity of **12** is associated with an improved antagonistic behaviour compared to the clinical candidate **1** (Table 1, Figure S10). The difference between **1** and **12** is especially pronounced for β-arrestin recruitment, where we detected a ≈10-fold increased potency for **12**. Moreover, **12** showed no inhibition of the related chemokine receptors CCR2 and CCR7 (Figure S11), indicating high CCR9 selectivity. With a high CCR9 selectivity, improved CCR9-affinity and antagonistic activity, the 4-aminopyrimidine **12** is an interesting new lead structure for further development. This is supported by the fact that the scaffold of **12** does not comprise the biaryl ketone substructure of **1**, which is considered a structural alert due to its reactivity.[15]

Since we have shown that the IABS of CCR9 tolerates the binding of heterobifunctional ligands, such as the TAMRA-labeled vercirnon analogue (**3a**), we were curious whether this binding site would serve as a suitable drug target site for heterobifunctional PROTACs as well. In general, PROTACs feature superior in vivo efficacy compared to standard inhibitors, which has been attributed to their catalytic mechanism and sustained pharmacological effects as a consequence of target protein degradation. The PROTAC approach has been widely applied by us and others to induce the degradation of cytosolic as well as membrane proteins, and first PROTACs have entered clinical trials, thereby highlighting the versatility and therapeutic potential of this concept.[16] For the design of CCR9-PROTACs, we considered the scaffolds of both **1** and **12**. As initial attempts to install a linker at the scaffold of **12** resulted in ligands with strongly reduced affinity, we proceeded with **1** for the design of CCR9-PROTACs.

Accordingly, we adapted the design and synthesis route that we successfully applied for the development of the vercirnon-based fluorescently labeled CCR9 ligands. For a proof-of-principle study, we conjugated an azido-functionalized CCR9 ligand with an alkynylated analogue of (*S*,*R*,*S*)-AHPC, to obtain a potential CCR9-PROTAC (**13**, Figure 4, Scheme S4). (*S*,*R*,*S*)-AHPC is a ligand for the recruitment of the von Hippel-Lindau (VHL) protein, an E3 ubiquitin ligase that has been frequently used for chemically induced protein degradation.[16a] Applying our NanoBRET-based binding assay, we showed that **13** is able to bind to the IABS of CCR9 with K_i values of 78.0 nM ($pK_i = 7.13 \pm 0.06$) and 151 nM ($pK_i = 6.86 \pm 0.08$) under membrane-based and cell-based conditions, respectively (Figure S12, Table S3). To investigate the effect of **13** on cellular CCR9 levels, we used an enzyme-linked immunosorbent assay (ELISA). In a range from 1–25 nM, **13** is able to reduce CCR9 levels in a concentration-dependent manner (Figure 4B). The observation that the maximum degradation effect of **13** was detected at concentrations below its cellular K_i value can be attributed to the catalytic mechanism of PROTACs. At higher PROTAC concentrations, we detected a reduced degradation efficacy. This observation, the so-called "hook effect", is typical for PROTACs and results from the formation of unproductive dimers at higher PROTAC concentrations rather than the productive ternary complex required for degradation.[16a] The epimeric negative control **14**, which is able to bind to CCR9 (Figure S12, Table S3) but unable to recruit VHL, exerted no CCR9 degradation (Figure 4C, S13A). Furthermore, we show that the effect of **13** on CCR9 degradation can be reduced by the NEDD8 activating E1 enzyme inhibitor MLN4924, which inhibits the process of ubiquitination and subsequent proteasomal degradation.[17] The degradation effect of **13** can be counteracted by competition with either **1** or (*S*,*R*,*S*)-AHPC. Single treatment with **1** or (*S*,*R*,*S*)-AHPC as well as their combination did not result in reduction of CCR9 levels (Figure 4C). In addition, **13** shows no cytotoxicity in HEK293T cells (Figure S13B) and selectively induces a reduction in CCR9 levels, without affecting the levels of the related chemokine receptors CCR2 and CCR7 (Figure S13C). Thus, our results strongly suggest that **13** is able to induce the proteasomal degradation of CCR9 and is therefore the first PROTAC targeting the IABS of GPCRs. Future studies will be directed towards the improvement of the degradation efficacy of CCR9-PROTACs and will investigate the functional consequences of CCR9 degradation.

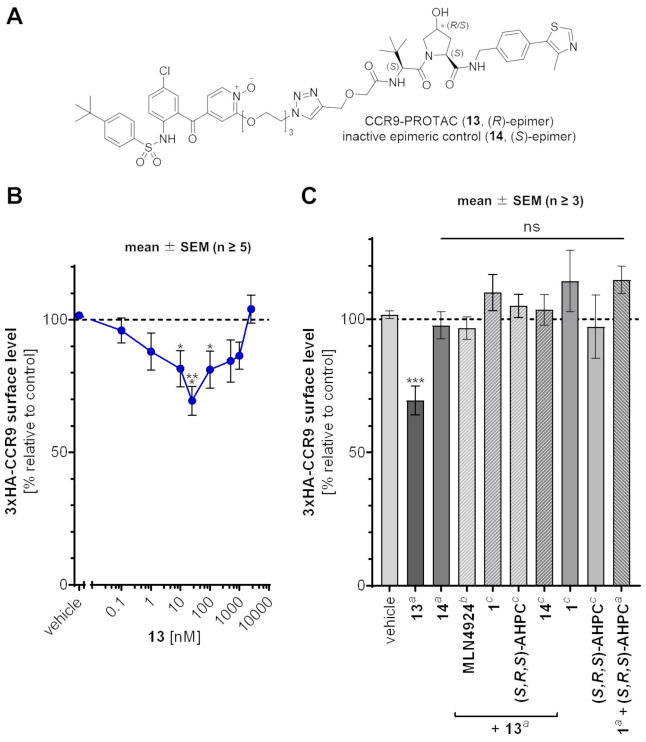

Figure 4. CCR9-PROTAC (**13**) induces the proteasomal degradation of CCR9 in HEK293T cells transiently expressing CCR9. A) Chemical structure of the CCR9-PROTAC **13** and its inactive epimer **14**. B) Quantification of the effect of **13** on CCR9 levels via ELISA at different compound concentrations. C) Control experiments with the inactive epimeric control **14**, the PROTAC constituents **1** and (*S*,*R*,*S*)-AHPC, as well as the NEDD8 activating E1 enzyme inhibitor MLN4924 validate that **13** reduces CCR9 levels by inducing the proteasomal degradation of CCR9. Compounds were tested at following concentrations: [a] 25 nM, [b] 3 μM, [c] 10 μM. Statistics (One-Way ANOVA): $*p \leq 0.05$, $***p \leq 0.0001$, all compared pairwise to a vehicle control.

In summary, by means of our fluorescent CCR9 ligand (**3a**), we report the development of the first small-molecule-based fluorescent probe targeting the IABS of GPCRs. This tool enabled thermodynamic and kinetic binding studies via the NanoBRET technique. Kinetic binding studies revealed that the interaction between CCR9 and the vercirnon scaffold is characterized by a long residence time, which rationalizes the high affinity and outstanding CCR9 selectivity of **1**. Furthermore, we showed that **3a** can be used for the identification of low molecular weight ligands (fragments), as well as for fluorescence microscopy as a tool to visualize intracellular ligand binding to CCR9. Applying our screening tool to membrane preparations and in living cells, we discovered the 4-aminopyrimidine analogue **12** as a new intracellular CCR9 antagonist with improved affinity and antagonistic activity compared to the clinical candidate **1**. To chemically induce CCR9 degradation, we developed the first PROTAC targeting the IABS of GPCRs. In a proof-of-principle study, we showed that our CCR9-PROTAC (**13**) is in fact able to reduce CCR9 abundance, thereby offering an unprecedented approach to modulate GPCR signal transduction.

Acknowledgements

M.E.H. (Do-L 205/05) and M.S. (Li 204/04) were supported by the Verband der Chemischen Industrie (VCI). D.W. receives funding from the Deutsche Forschungsgemeinschaft (DFG, GRK1910). Microscopy was performed at the Optical Imaging Centre Erlangen (OICE), funded by the Deutsche Forschungsgemeinschaft (DFG, 441730715). We thank A.A. Aziz and V. Kapferer for the assistance with compound synthesis, the Erlangen Regional Computing

Center (RRZE) for compute resources and support, and Prof. Peter Gmeiner for supervising M.F.S. and for mentoring and hosting the research of M.S. Open Access funding enabled and organized by Projekt DEAL.

Conflict of Interest

The authors declare no conflict of interest.

Data Availability Statement

The data that support the findings of this study are available in the Supporting Information of this article.

Keywords: CCR9 · Drug Design · Fluorescent Probes · PROTAC · Receptors

[1] Y. Zheng, L. Qin, N. V. Ortiz Zacarìas, H. de Vries, G. W. Han, M. Gustavsson, M. Dabros, C. Zhao, R. J. Cherney, P. Carter, D. Stamos, R. Abagyan, V. Cherezov, R. C. Stevens, A. P. Ijzerman, L. H. Heitman, A. Tebben, I. Kufareva, T. M. Handel, *Nature* **2016**, *540*, 458–461.

[2] K. Jaeger, S. Bruenle, T. Weinert, W. Guba, J. Muehle, T. Miyazaki, M. Weber, A. Furrer, N. Haenggi, T. Tetaz, C.-Y. Huang, D. Mattle, J.-M. Vonach, A. Gast, A. Kuglstatter, M. G Rudolph, P. Nogly, J. Benz, R. J. P. Dawson, J. Standfuss, *Cell* **2019**, *178*, 1222–1230.

[3] C. Oswald, M. Rappas, J. Kean, A. S. Doré, J. C. Errey, K. Bennett, F. Deflorian, J. A. Christopher, A. Jazayeri, J. S. Mason, M. Congreve, R. M. Cooke, F. H. Marshall, *Nature* **2016**, *540*, 462–465.

[4] X. Liu, S. Ahn, A. W. Kahsai, K.-C. Meng, N. R. Latorraca, B. Pani, A. J. Venkatakrishnan, A. Masoudi, W. I. Weis, R. O. Dror, X. Chen, R. J. Lefkowitz, B. K. Kobilka, *Nature* **2017**, *548*, 480–484.

[5] N. V. Ortiz Zacarías, E. B. Lenselink, A. P. IJzerman, T. M. Handel, L. H. Heitman, *Trends Pharmacol. Sci.* **2018**, *39*, 547–559.

[6] M. J. Walters, Y. Wang, N. Lai, T. Baumgart, B. N. Zhao, D. J. Dairaghi, P. Bekker, L. S. Ertl, M. E. T. Penfold, J. C. Jaen, S. Keshav, E. Wendt, A. Pennell, S. Ungashe, Z. Wei, J. J. K. Wright, T. J. Schall, *J. Pharmacol. Exp. Ther.* **2010**, *335*, 61–69.

[7] a) E. Wendt, S. Keshav, *Clin. Exp. Gastroenterol.* **2015**, *8*, 119–130; b) B. G. Feagan, W. J. Sandborn, G. D'Haens, S. D. Lee, M. Allez, R. N. Fedorak, U. Seidler, S. Vermeire, I. C. Lawrance, A. C. Maroney, C. H. Jurgensen, A. Heath, D. J. Chang, *Aliment. Pharmacol. Ther.* **2015**, *42*, 1170–1181.

[8] a) T. R. Chan, R. Hilgraf, K. B. Sharpless, V. V. Fokin, *Org. Lett.* **2004**, *6*, 2853–2855; b) R. Huisgen, *Proc. Chem. Soc. London* **1961**, 357–396.

[9] M. P. Hall, J. Unch, B. F. Binkowski, M. P. Valley, B. L. Butler, M. G. Wood, P. Otto, K. Zimmerman, G. Vidugiris, T. Machleidt, M. B. Robers, H. A. Benink, C. T. Eggers, M. R. Slater, P. L. Meisenheimer, D. H. Klaubert, F. Fan, L. P. Encell, K. V. Wood, *ACS Chem. Biol.* **2012**, *7*, 1848–1857.

[10] R. A. Copeland, *Nat. Rev. Drug Discovery* **2016**, *15*, 87–95.

[11] S. B. Kalindjian, S. V. Kadnur, C. A. Hewson, C. Venkateshappa, S. Juluri, R. Kristam, B. Kulkarni, Z. Mohammed, R. Saxena, V. N. Viswanadhan, J. Aiyar, D. McVey, *J. Med. Chem.* **2016**, *59*, 3098–3111.

[12] A. J. M Zweemer, I. Nederpelt, H. Vrieling, S. Hafith, M. L. J. Doornbos, H. de Vries, J. Abt, R. Gross, D. Stamos, J. Saunders, M. J Smit, A. P Ijzerman, L. H. Heitman, *Mol. Pharmacol.* **2013**, *84*, 551–561.

[13] J. Zhang, J. Romero, A. Chan, J. Goss, S. Stucka, J. Cross, B. Chamberlain, M. Varoglu, H. Chandonnet, D. Ryan, B. Lippa, *Bioorg. Med. Chem. Lett.* **2015**, *25*, 3661–3664.

[14] J. A. Ballesteros, H. Weinstein in *Methods in Neurosciences* (Ed.: C. S. Stuart), Academic Press, New York, **1995**, pp. 366–428.

[15] N. Narita, A. Morohashi, K. Tohyama, T. Takeuchi, Y. Tagawa, T. Kondo, S. Asahi, *Drug Metab. Dispos.* **2018**, *46*, 204–213.

[16] a) G. M. Burslem, C. M. Crews, *Cell* **2020**, *181*, 102–114; b) M. Schiedel, D. Herp, S. Hammelmann, S. Swyter, A. Lehotzky, D. Robaa, J. Oláh, J. Ovádi, W. Sippl, M. Jung, *J. Med. Chem.* **2018**, *61*, 482–491.

[17] T. A. Soucy, P. G. Smith, M. A. Milhollen, A. J. Berger, J. M. Gavin, S. Adhikari, J. E. Brownell, K. E. Burke, D. P. Cardin, S. Critchley, C. A. Cullis, A. Doucette, J. J. Garnsey, J. L. Gaulin, R. E. Gershman, A. R. Lublinsky, A. McDonald, H. Mizutani, U. Narayanan, E. J. Olhava, S. Peluso, M. Rezaei, M. D. Sintchak, T. Talreja, M. P. Thomas, T. Traore, S. Vyskocil, G. S. Weatherhead, J. Yu, J. Zhang, L. R. Dick, C. F. Claiborne, M. Rolfe, J. B. Bolen, S. P. Langston, *Nature* **2009**, *458*, 732–736.

Manuscript received: December 8, 2021
Accepted manuscript online: December 22, 2021
Version of record online: January 27, 2022